Potential for Multi-Functional Additive Manufacturing Using Pulsed Photonic Sintering

Sourav Das, Denis Cormier, and Scott Williams

Rochester Institute of Technology, New York, U.S.
sxd6026@rit.edu, cormier@mail.rit.edu, sawppr@rit.edu

Abstract

This paper proposes the integration of pulsed photonic sintering into multi-material additive manufacturing processes in order to produce multifunctional components that would be nearly impossible to produce any other way. Pulsed photonic curing uses high power Xenon flash lamps to thermally fuse printed nanomaterials such as conductive metal inks. To determine the feasibility of the proposed integration, three different polymer additive manufacturing materials were exposed to typical flash curing conditions using a Novacentrix Pulseforge 3300 system. FTIR analysis revealed virtually no change in the polymer substrates, thus indicating that the curing energy did not damage the polymer. Next, copper traces were printed on the same substrate, dried, and photonically cured to establish the feasibility of thermally fusing copper metal on the polymer additive manufacturing substrates. Although drying defects were observed, electrical resistivity values ranging from 0.081 to 0.103 Ω/sq. indicated that high temperature and easily oxidized metals can be successfully printed and cured on several commonly used polymer additive manufacturing materials. These results indicate that pulsed photonic curing holds tremendous promise as an enabling technology for next generation multi-material additive manufacturing processes.

Keywords: 3D printing, additive manufacturing, functional printing, printed electronics, photonic curing

1 Introduction

The phrase "multi-functional additive manufacturing" describes processes capable of incorporating a variety of material types within a component such that the resulting component has a higher degree of functionality than would normally be found in a purely mechanical part. For example, a process might print actuator materials that connect moving components in an assembly. Embedded heaters might be printed that dynamically modify mechanical properties of a material. Strain gauges printed on or within a component could provide data for structural health monitoring.

Relatively few commercial systems are able to spatially control material composition throughout a component at this time. A comprehensive literature survey of multi-material

additive manufacturing research (Vaezi *et al.*, 2013) suggests that multi-material additive manufacturing is still primarily in the research domain. As multi-material AM research approaches are incorporated into commercially available technologies in the coming years, the integration of metal, polymer, and even ceramic materials within the same component may ultimately prove to be the most transformative aspect of additive manufacturing technologies with respect to traditional manufacturing techniques. Engineers will be able to optimize functional performance of components in ways never before envisioned.

Some of the earliest embodiments of multi-functional additive manufacturing involved the integration of electronics on or within an additively manufactured component. For example, Periard *et al.* (2007) used a syringe paste extrusion system to demonstrate conductive silver ink deposition for fabrication of demonstration objects such as a flashlight and a blinking LED circuit. Johnson *et al.* (2011) direct-write printed multiple layers of materials, including photopolymers and silver inks, to produce a MEMS micropump suitable for delivering drugs to the inner ear. Lopes *et al.* (2012) describe a hybrid additive manufacturing configuration in which an nScrypt direct-write micro- dispensing nozzle was integrated with a 3D Systems SLA 250 stereolithography system to produce items in which conductive silver traces are embedded within the SLA photopolymer resin.

These three examples help demonstrate the potential of multi-material additive manufacturing technologies. One important item to note, however, is that the overwhelming majority of multi- material additive manufacturing research involving both polymers and metals in the same part use silver as the metallic material. The simple reason for this is that metals and polymers generally have incompatible processing temperatures. Silver nanoparticle inks and pastes, however, can be cured at relatively low temperatures (<150C) without any need for protective or reducing atmospheres.

While silver is very well suited as an electrical conductor material, technologies capable of processing a wider range of metal and polymeric materials within the same component are needed if the promise of multi-functional additive manufacturing is to be realized. Technologies used in the printed electronics industry have much to offer in this regard. Printed electronics often require metallic electrode layers deposited onto polymeric substrates such as polyethylene terephthalate (PET), polycarbonate, or polyimide (Kapton). While silver is frequently used for the reasons mentioned above, recent as-yet published research with pulsed photonic curing of higher temperature metals such as copper, stainless steel, and nickel from the author's lab shows promise for applications in multi-functional additive manufacturing.

Pulsed photonic curing (Schroder *et al.*, 2006) is a relatively new process in which printed nano-inks are cured or sintered using flashes of broad spectrum light energy from Xenon lamps. Functional inks are typically printed on a substrate using screen printing, flexography, inkjet printing, or other suitable processes. The printed film passes beneath one or more high power Xenon lamps, and the power, pulse length, number of pulses, and pulse frequency are chosen to optimally cure or sinter the material without thermally damaging the bulk substrate material (Figure 1).
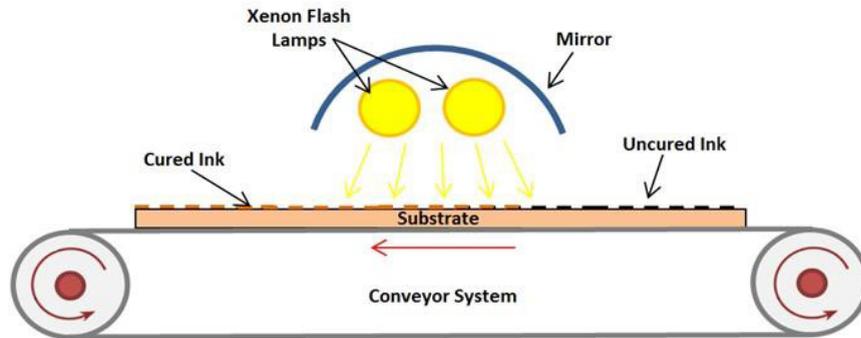
Figure 1: Pulsed photonic curing

A key aspect of pulsed photonic curing is the well-known phenomenon of melting/sintering point depression in nanoparticles described by the Gibbs-Thomson equation (Makkonen, 2000)

$$T_M(d) = T_{MB}\left(1 - \frac{4\sigma_{SL}}{H_f\rho_s d}\right)$$

$T_M(d)$ is the depressed melting temperature of nanoparticles of diameter d, T_{MB} is the material's bulk melting temperature, σ_{SL} is the solid-liquid interface energy, H_f is the bulk heat of fusion, and ρ_s is the density of solid material. As d gets below approximately 50 nm, dramatic reductions in the thermal processing temperature are observed. This makes it possible to rapidly fuse high temperature metals on low temperature polymers at very high speeds. For example, Farnsworth et al. (2012) describe the use of photonic curing for printed RFID tags as well as thin-film transistors on polymer substrates. Reinhold et al. (2013) describe recent advances in high speed pulsed photonic curing of copper oxide inks printed on low temperature polymer or even paper substrate materials for printed electronics. The fact that the Xenon lamps emit a broad spectrum of energy is also particularly attractive due to the fact that each potential functional material of interest has specific absorption characteristics. Pulsed photonic curing is therefore very flexible in terms of the range of materials that can be thermally processed when compared with single wavelength sources such as scanning lasers.

While pulsed photonic curing has been explored for flexible electronics on Kapton, PET, and paper substrates, this paper proposes its use as the energy source in multi-material additive manufacturing systems capable of printing both polymer and metal materials within the same component. Although a handful of researchers have investigated the use of silver conductive ink on or in 3D printed polymer parts, we are unaware of any efforts to date that investigate the feasibility of integrating higher temperature reactive inks within a 3D printed component. We are also unaware of any efforts to use high speed broad spectrum curing within an additive manufacturing process. Lastly, the potential for thermally or photonically induced damage to the polymer during photonic curing has never been studied.

In order to assess the technical viability of the proposed approach, two fundamental questions must first be answered:

1. Is it possible to fuse printed high temperature metal inks on commonly used additive manufacturing polymers?

2. Are commonly used additive manufacturing polymers damaged by the incident energy?

The remainder of this paper is dedicated to answering these two questions.

2 Materials and Methods

To determine whether or not energy from the Xenon flash lamps cause damage to the polymer substrates, sample substrate specimens were prepared for the stereolithography (SLA), selective laser   sintering (SLS), and fused deposition modeling (FDM) processes. For the SLA process, DSM Somos NanoTool substrate specimens were produced on a 3D Systems Viper SLA machine. For the SLS process, PA 2201 (polyamide) substrate specimens were produced on an EOS P730 system. Lastly, ABSPlus substrate specimens were produced on a Dimension Elite system from Stratasys. It would be impractical to test every polymer additive manufacturing material; however the three process/material   combinations chosen for this evaluation are reasonably representative of an extremely large percentage   of polymer additive manufacturing materials used in practice.

One specimen of each material type was set aside as an "as processed" control sample. One additional specimen of each type was then passed through a Novacentrix Pulseforge 3300 machine (Figure 2) such that the bare polymer would be exposed to the incident energy. The PulseForge 3300 tool is capable of delivering peak powers as high as 100 kW/cm^2 in pulses as short as 30 microseconds. For this work, each sample was exposed to two 270 V pulses having a duration of 1370 microseconds at a pulse frequency of 2.8 Hz. These pulse conditions are representative of what a polymer substrate would be exposed to when copper ink is thermally cured via this process. The pairs of as-processed and photonically cured samples were then examined via FTIR analysis using a BioRad Excaliber FTS 3000 FTIR with 4 cm^{-1} resolution to determine whether any appreciable changes in the   molecular structure could be detected. The use of FTIR for this purpose was suggested by Celina *et al* (1997) who conducted a study in which FTIR spectra for a variety of thermally processed polymer specimens were found to be good indicators of thermally induced damage (or lack thereof).

After bare substrates were examined for potential adverse effects, Novacentrix Metalon ICI-021 aqueous dispersion copper oxide ink with 62% solid loading fraction was screen printed onto new sets of additively manufactured polymer substrates. A 203 mm x 254 mm (8 in. x 10 in.) aluminum frame was used with a 280 mesh screen and a wire diameter of 25.4 μm (0.001 in.). Screen printing was specifically used, as it allowed large numbers of samples to be printed almost simultaneously so that every sample could be printed, dried, and then cured in the same amount of time before conductivity readings were taken. This is important, as factors such as drying time have been known to influence conductivity for many ink formulations.

Figure 2: Novacentrix Pulseforge 3300

The geometry shown in Figure 3 was used to allow conductivity measurements of cured samples to be taken. All samples were oven dried for 3 minutes at 150 °C prior to photonic curing. They were then photonically cured on the Novacentrix PulseForge 3300 using the same pulse settings as previously described for the bare substrates. Copper is the dominant conductive circuit board material, hence it makes the ideal test case for multi-functional additive manufacturing that includes both metal and polymer materials within the same component.
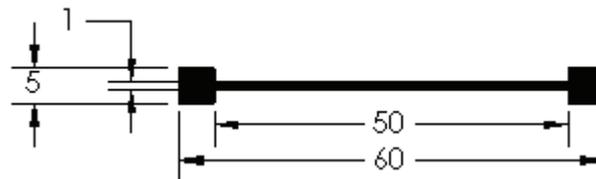
**Figure 3:** Conductivity coupon geometry (units: mm)

3 Results

3.1 FTIR Results

As described in Section 2, FDM, SLS, and SLA samples were passed through a PulseForge 3300 under the same processing conditions used to cure printed copper ink. This was done to determine whether or not the energy from the Xenon lamps is sufficiently high to cause damage to any of the most commonly used AM polymers.

Figure 4 shows the FTIR spectra for as-printed and photonically cured PA2201 (polyamide) processed in the EOS P730 system. Figure 5 shows the FTIR spectra for as-printed and photonically cured ABSPlus material processed in the Dimension Plus FDM system.

Lastly, Figure 6 shows the FTIR spectra for as-printed and photonically cured NanoTool resin cured in the 3D Systems Viper SLA machine. In all three graphs, a dashed line represents response of the as-printed polymer, and the solid line represents the response of the photonically cured material.

In the cases of the white PA2201 (Fig. 4) and white NanoTool resin (Fig. 6), the two curves are almost perfectly superimposed. This provides one indicator that the processing conditions used to cure copper caused little, if any, appreciable damage to these commonly used additive manufacturing polymer materials. ABS plastic used in FDM machines is available in a variety of colors including black, white, red, green, blue, yellow, and green. Black ABS was intentionally chosen for this study due to the case that it represents a "worst case scenario" in the sense that it will absorb nearly all wavelengths emitted by the Xenon lamps and would therefore be most likely to show thermal damage. As seen in Figure 5 for the black ABS, there is a slight downward shift in the spectra between roughly 500-1300 cm^{-1}. Referring to the black ABS sample seen in Figure 7, one can detect a slightly duller appearance of the black ABS that has been photonically cured (left side). The FTIR spectra and slight visual difference suggest slight thermal damage at the surface of the dark black material.
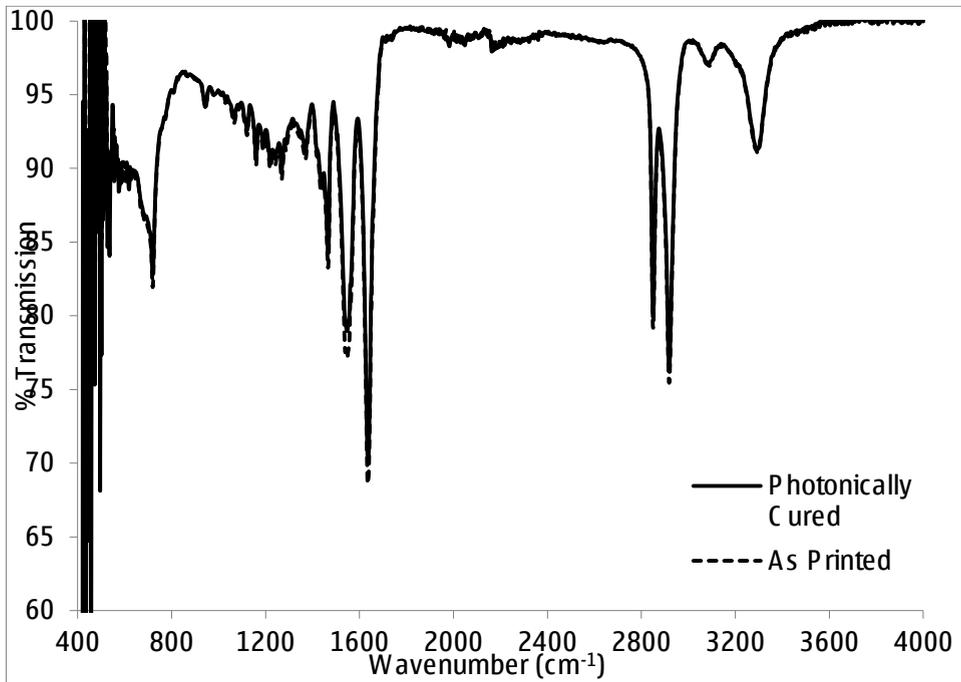
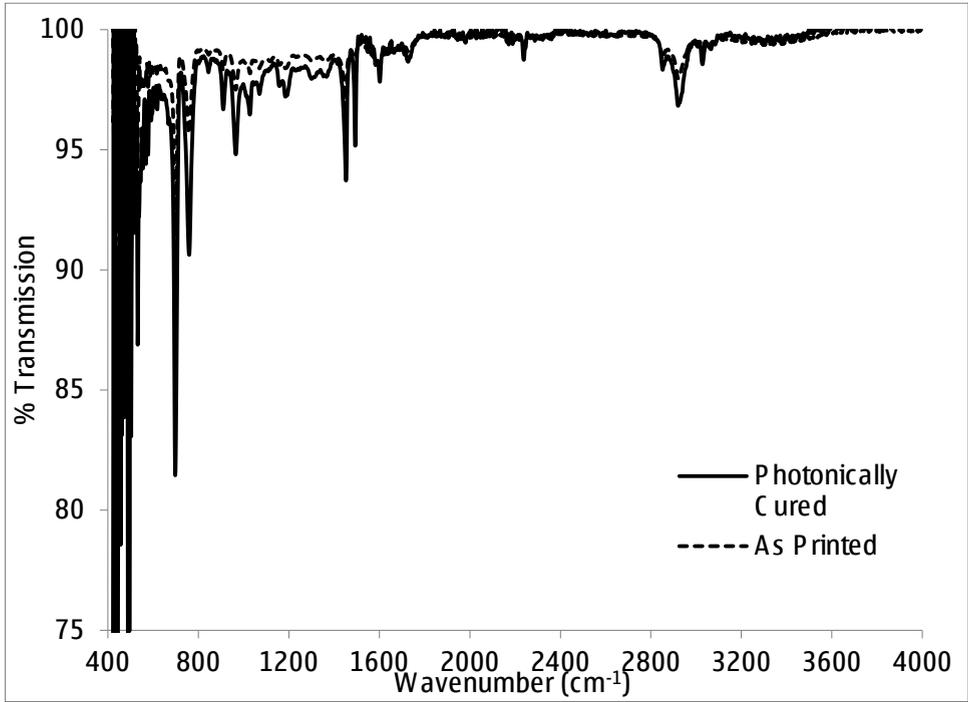**Figure 4:** FTIR analysis of PA2201 samples produced in an EOS P730 SLS machine

371

Figure 5: FTIR analysis of black ABSPlus samples produced in a Dimension Elite FDM machine
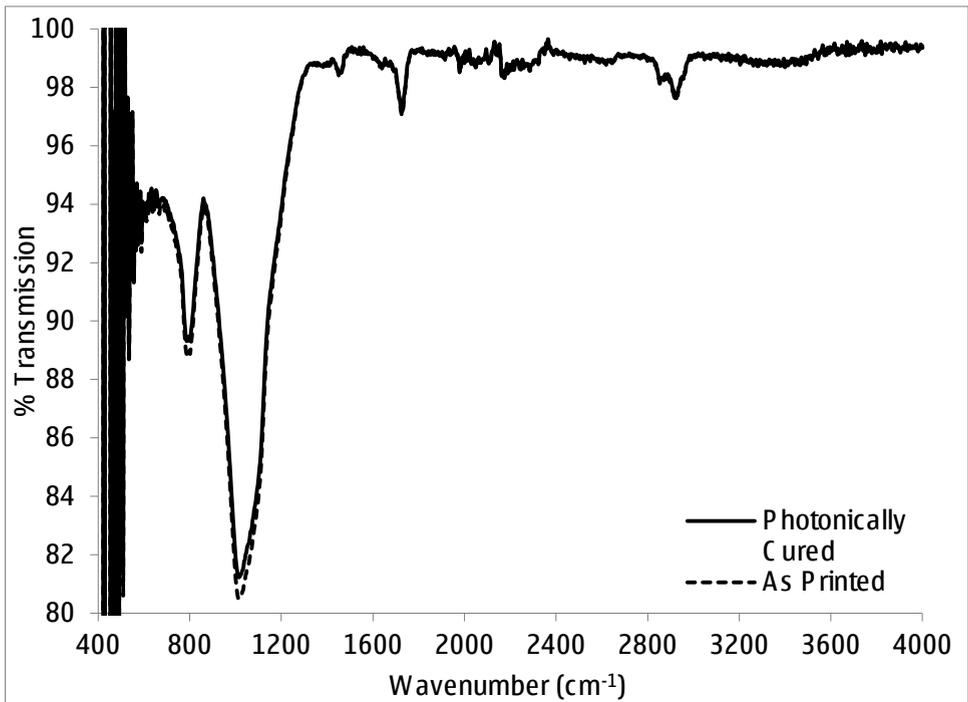

Figure 6: FTIR analysis of NanoTool resin samples produced using a 3D Systems Viper SLA machine

3.2 Photonic Curing of Copper on Polymer Substrates

Copper oxide paste was screen printed, dried, and photonically cured on polymer substrates according to the methods described Section 2. A minimum of 6 samples were prepared for each substrate type in order to provide statistically useful results. Figure 7 shows FDM and SLS samples with both as-printed (dark color) and photonically cured (copper color) material. This particular conductive ink uses copper oxide nanoparticles and flake along with a proprietary reducing agent. Upon passing through the photonic curing system, the non-conductive copper oxide reduces to conductive copper.

After photonic curing, each sample's resistivity was measured using a Fluke 115 multimeter. Each trace was 50 mm long and 1 mm wide, giving a conductive length of 50 squares. Average resistivity of cured copper on the ABSPlus samples was 0.1048 ± 0.0023 Ω/sq. Average resistivity of cured copper on PA2201 (nylon) was 0.0976 ± 0.0013 Ω/sq. Average resistivity of cured copper on Somos NanoTool was 0.0813 ± 0.0070 Ω/sq. In separate testing unrelated to this research, conductivities of 0.035-0.050 Ω/sq have typically been obtained with the same screen printed copper paste on paper substrates. While the resistivity on the three additive manufacturing polymers is not as low as those seen with paper substrates, these values are generally quite acceptable for general purpose applications in which conductive traces connecting power sources, LED's, small motors, and other components are used.
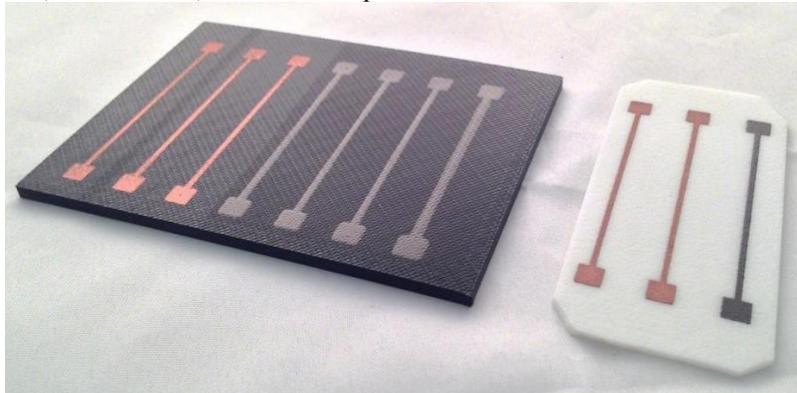

Figure 7: Screen printed copper (dark color) and photonically cured copper (bright color) on polymer AM substrates

4 Discussion

When samples are photonically cured, the pulse power, pulse duration, frequency, etc. are controlled in order to produce the desired surface heating without overheating the substrate. Simpulse is a one-dimensional heat transfer simulation module that comes with the PulseForge tool that allows users to simulate the pulsed photonic curing process. It includes surface convection and radiation terms. Users specify the material being cured, the substrate material(s), and the thicknesses of each material. Thermophysical material properties including mass density (ρ), conductivity (κ), and specific heat (c_p) of each material must also be specified. The user then specifies the photonic curing processing conditions to be simulated. These include the pulse voltage, pulse duration, number of pulses, and pulse frequency. SimPulse then simulates the heat profile through the thickness of the

stack.

Figure 8 shows results of a Simpulse study for a 30 μm thick layer of Novacentrix Metalon copper oxide nanoparticle ink on top of 3 mm thick ABS plastic. This approximates the screen printed copper oxide and FDM ABS plastic thicknesses for the physical samples used in experimental testing. The mass density (ρ), conductivity (κ), and specific heat (c_p) were taken to be 6.00 g/cm3, 0.2 W/m-K, and 448 J/kg-K respectively for the printed copper oxide ink, and 1.04 g/cm3, 0.17 W/m-K, and 1400 J/kg-K respectively for ABS plastic. The photonic curing process parameter values of two pulses at 270 volts/pulse, 1370 msec per pulse, and a pulse frequency of 2.8 Hz were then specified. After inputting the above settings into SimPulse, estimated time versus temperature profile through the thickness of the stack was generated. Figure 8 shows temperature versus time at 2 locations. The red (top) curve shows temperature on the top surface of the printed copper oxide trace, while the blue (lower) curve shows temperature on top of the ABS plastic. Two important observations can be made. The copper oxide ink exhibits very rapid, though brief heating to just over 600°C. The ABS plastic, however, never exceeds 150°C. Even at peak temperature, the ABS cools down to below 100C within approximately 25 msec. Although Simpulse is based upon a relatively simple model for temperature estimation only, these results tend to add further evidence beyond FTIR measurements that intense, but brief, bursts of broad spectrum energy have considerable potential for high speed thermal processing of high temperature materials on or in polymeric 3D printed components.
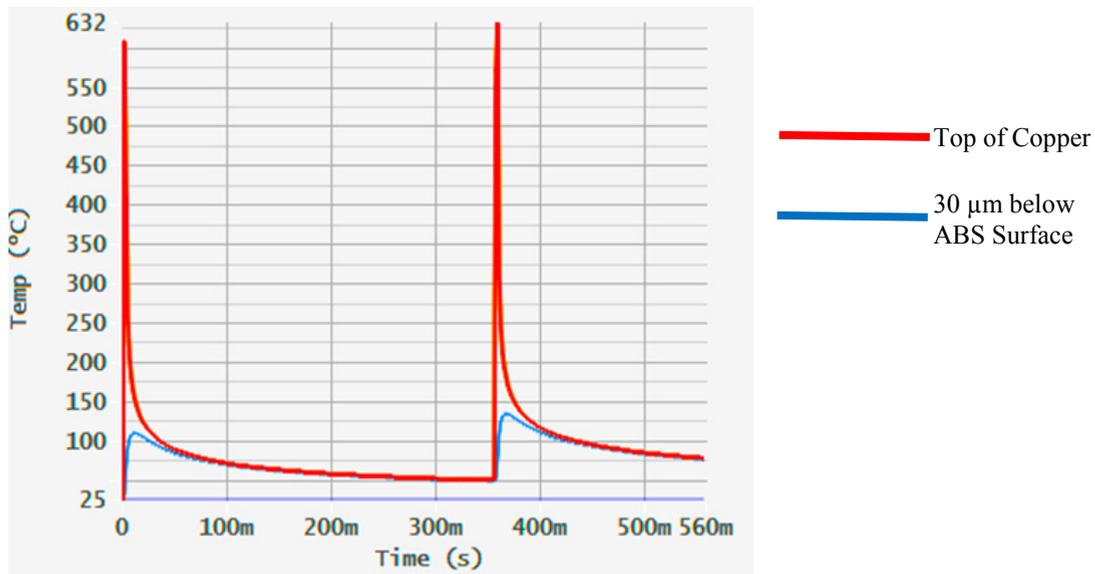
**Figure 8:** Temperature versus time for photonically cured copper on ABS substrate

The resistivity values reported in Section 3.2 are quite acceptable for a wide range of printed electronics applications, and the average resistivity for the ABS and PA2201 samples were reasonably close. It is worth noting, however, that considerably greater variability in resistivity was seen in the PA2201 samples than with the ABSPlus. Upon closer inspection of the samples via optical microscopy, pronounced differences between the samples were observed. Figures 9, 10, and 11 show as-printed, dried, and photonically cured copper on the ABSPlus, PA2201, and Nanotool substrates respectively. Figures 9(c), 10(c), and 11(c) are intentionally arranged from highest to lowest electrical resistivity for purposes of qualitative visual comparison.

In Figure 9, the printed tracks associated with extruded black ABS filament are plainly visible.

It is   readily apparent that the copper formed cracks along the gaps between the printed tracks. It can also be   seen that the dried copper trace is considerably wider than the 1 mm wide track produced by the screen printer. The saw tooth pattern shows where copper wicked into the gaps between printed tracks during drying. In some areas, the drying cracks span nearly the entire width of the printed copper trace and   clearly explain the lower conductivity compared with the SLS and SLA samples.

   A different phenomenon is seen in Figure 10. Surfaces produced in the Selective Laser Sintering process have a grainy, but solid, surface texture. Although the SLS samples do not suffer from long continuous drying cracks as seen in the FDM samples, a multitude of shorter randomly oriented drying cracks that disrupt the conductive path are plainly visible.
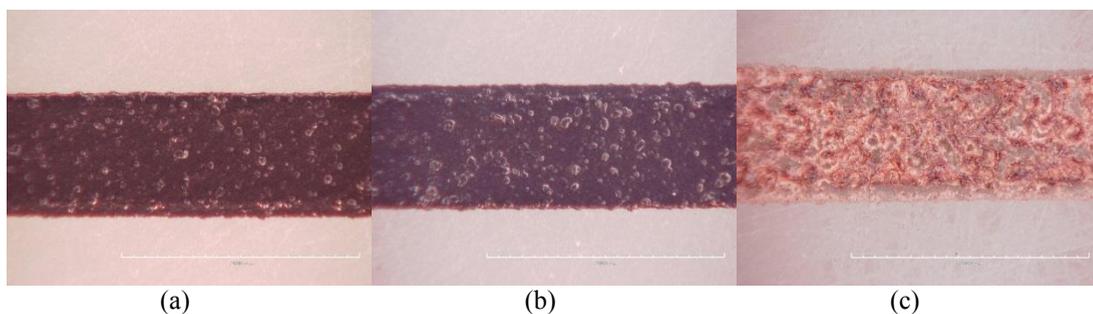
   Figure 11 shows a micrograph of cured copper on the Somos NanoTool substrate. This copper had   the lowest electrical resistivity, or conversely the highest electrical conductivity, of all samples. While the cured material is sponge-like due to gas evolving from the copper oxide reduction reaction during curing, it does not have the macro-scale cracks that are readily visible in the FDM and SLS samples. It is worth noting that the Somos NanoTool resin has considerably lower coefficient of thermal expansion than the other two materials studied. Specifically, the coefficients of thermal expansion are given as 88.2 μm/μm/°C, 62.3 μm/μm/°C, and 31.4 μm/μm/°C for ABSPlus, PA2201,   and Somos NanoTool data sheets respectively. Thus differences between the thermal expansion of the substrate and printed ink during pulsed photonic curing is considered to play a significant role in the formation of microcracks. Nevertheless, sheet resistivity values ranging from 70-105 mΩ/sq is reasonable for a broad range of applications.

| (a) | (b) | (c) |
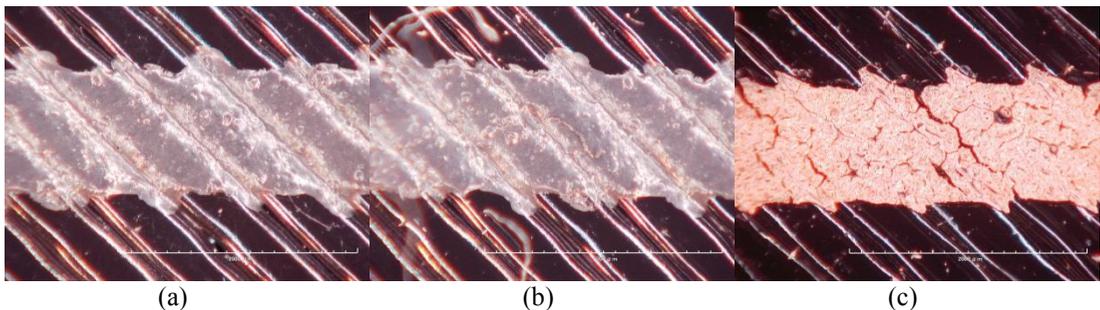
Figure 9: Micrograph of (a) as-printed, (b) dried, and (c) photonically cured copper on black ABSPlus substrate

| (a) | (b) | (c) |
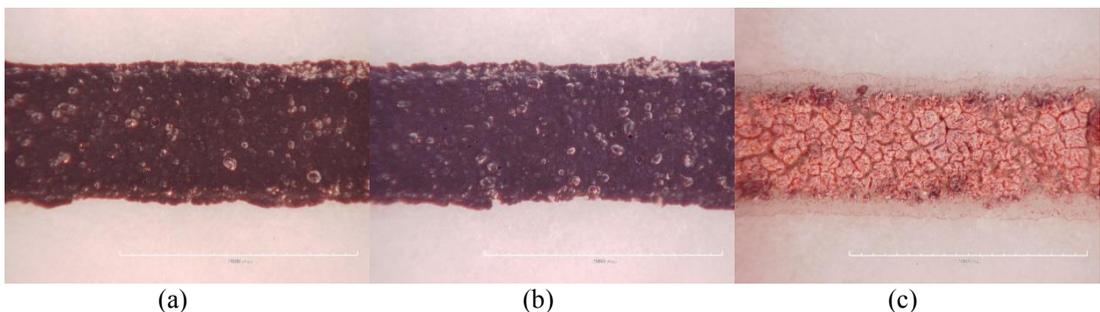
Figure 10: Micrograph of (a) as-printed, (b) dried, and (c) photonically cured copper on PA2201 substrate

(a)   (b)   (c)

Figure 11: Micrograph of (a) as-printed, (b) dried, and (c) photonically cured copper on SLA Nanotool substrate

5 Summary and Conclusions

This paper explores the use of pulsed photonic curing as a potential path to multifunctional 3D printing in which a broad range of material types may be combined within the same component. The first objective of the paper was to determine whether or not pulsed photonic curing damages the polymer structure. FTIR analysis did not indicate any appreciable change in the polymer structure. Furthermore, a simple 1-D thermodynamic simulation model supports the notion that although the copper oxide nanoparticles achieve high temperatures for brief amounts of time, the polymer substrate temperature does not exceed approximately 150 °C and is only above roughly 100 °C for on the order of 25 msec.

The second objective of the study was to observe behavior of photonically cured high temperature material (copper in this case) on three representative polymers – an amorphous thermoplastic (ABS), a crystalline thermoplastic (polyimide), and a UV curable resin (NanoTool). Electrical resistivity ranged from 0.007 to 0.105 Ω/sq for the three materials. Micrographic examination of the copper on each of the three substrate materials revealed significant differences. The black ABS substrates produced via the FDM process exhibited substantial wicking and cracking of the copper paste along the gaps between adjacent printed traces. This would indicate that post processing of FDM components to smooth and seal the surfaces is advised. For instance, solvent vapor smoothing with acetone is a simple method that is often used. The polyamide SLS substrate did not exhibit macro cracking of the same magnitude as the ABS samples, however, a large number of smaller cracks were visible which would adversely affect conductivity. The very smooth SLA Nanotool substrates had the lowest resistivity of all samples. That material also had the lowest coefficient of thermal expansion.

In summary, this study suggests that pulsed photonic is very promising with respect to multifunctional 3D printing. A system is currently under development in which multi-material digital printing is integrated with the photonic curing system to produce multifunctional 3D printed components. In parallel with this development work, efforts are also underway to develop a database of material compatibilities that designers will refer to when selecting multiple materials that are incorporated into a given 3D printed device. Factors to consider, for example, include surface energy, viscosity, polarity, adhesion, coefficient of thermal expansion, and galvanic potential.

References

Celina, M., Ottesen, D., Gillen, K., and Clough, R. FTIR emission spectroscopy applied to polymer degradation. *Polymer degradation and stability* 1997; 58(1), 15-31.

Farnsworth, S., Schroder, K., Wenz, B., Pope, D., and Rawson, I. The Photonic Curing Process for Printed Electronics with Applications to Printed RFID Tags and Thin Film Transistors. In: *NIP & Digital Fabrication Conference,* 2012, no. 2, 440-443.

Johnson, D., Getpreecharsawas, J., Balasubramanian, S., Datar, A., Cormier, D., and Borkholder, D. Hybrid MEMS: extending micro manufacturing with direct write processes. In: *Technical Digest of Transducers Research Foundation Technologies for Future Micro-Nano Manufacturing Workshop* 2011.

Lopes, A., MacDonald, E., and Wicker, R. Integrating stereolithography and direct print technologies for 3D structural electronics fabrication. *Rapid Prototyping Journal* 2012; 18(2), 129 – 143.

Makkonen, L. On the methods to determine surface energies. *Langmuir*, 2000; 16(20), 7669-7672.

Periard, D., Malone, E., and Lipson, H. Printing embedded circuits. In: *Proceedings of the 18th Solid Freeform Fabrication Symposium,* 2007, pp. 503-12.

Reinhold, I., Voit, W., Rawson, I., Martin, K., Pope, D., Farnsworth, S., Zapka, W., and Munson C. Novel Developments in Photonic Sintering of Inkjet Printed Functional Inks, In: *NIP & Digital Fabrication Conference*, 2013, no. 2, 476-478.

Schroder, K., McCool, S., and Furlan, W. Broadcast photonic curing of metallic nanoparticle films. *Presented at NSTI Nanotech* 2006, 11.

Vaezi, M., Chianrabutra, S., Mellor, B. and Yang, S. Multiple material additive manufacturing – Part 1: a review. *Virtual and Physical Prototyping*, 2013; 8(1), 19-50.

Wilson, J., and Shin, Y. C. Microstructure and wear properties of laser-deposited functionally graded Inconel 690 reinforced with TiC. *Surface and Coatings Technology*, 2012; 207, 517-522.